MODELLING HOURLY SPATIO-TEMPORAL $PM_{2.5}$ CONCENTRATION IN WILDFIRE SCENARIOS USING DYNAMIC LINEAR MODELS

Joseph Sánchez-Balseca[a*], Agustí Pérez-Foguet[a]

[a]Research group on Engineering Sciences and Global Development (EScGD),

Civil and Environmental Engineering Department,

Universitat Politècnica de Catalunya – BarcelonaTech (UPC), Spain.

*Corresponding author: (+34) 690 132 602. Jordi Girona 31, UPC Campus Nord 08034, Barcelona, Spain.

E-mail address: joseph.sanchez@upc.edu, agusti.perez@upc.edu

HIGHLIGHTS

- $PM_{2.5}$ exposure can be obtained even at sites with no monitoring stations.
- Remotely sensed data can be used for spatial prediction on air quality modelling.
- Thermal anomalies are important to modelling air quality at wildfire scenarios.
- $PM_{2.5}$/ PM_{10} ratio could be used in areas with limited monitoring stations.

ABSTRACT

Particulate matter with aerodynamic diameter <2.5 μm ($PM_{2.5}$) is one of the main pollutants generated in wildfire events with negative impacts on human health. In research involving wildfires and air quality, it is common to use emission models. However, the commonly used emission approach can generate errors and contradict the empirical data. This paper adopted a statistical approach based in evidence of ground level monitoring and satellite data. An hourly $PM_{2.5}$ spatio-temporal model based on a dynamic linear modelling framework with Bayesian approach was proposed in a territorial context with a reduced number of monitoring stations for particulate matter.

The model validation is complicated by the fact that all monitoring stations are used in the model calibration. The novel validation method proposed considered both the particulate matter with aerodynamic diameter <10 μm (PM_{10}) recorded as daily value from 24-h mean every six days as well as the $PM_{2.5}/PM_{10}$ ratio. Modelling was carried out to provide satisfactorily the exposure level of $PM_{2.5}$ in a case study of wildfire event.

Keywords: Wildfire; Spatial modelling; Environmental statistics; Air quality; Particulate matter.

1. Introduction

Wildfires are an ecological disturbance with climatic, social and economic impacts on a global, regional and local scale (Amraoui et al., 2015; Hirschberger, 2016; Nunes et al., 2016). Wildfires are a natural significant source of air pollution (Smith, 1990; Bravo et al., 2002; Sapkota et al., 2005). Wildfire emissions can be higher than those emitted by specific activity sectors (e.g., the transport sector). However, wildfire emissions are released into the atmosphere only a few times during short periods (Martins et al., 2012). Particulate matter from wildfires is highly visible, affects ambient air quality, and has various effects on human health (Ward and Smith, 2005; Reinhardt et al., 2001; Knorr et al., 2012; Fann et al., 2018). Much of the increase in PM concentration during wildfires is primarily observed in the fine fraction ($PM_{2.5}$) (Sapkota et al., 2005; Mathur, 2008).
$PM_{2.5}$ from wildfires has the greatest effect on visibility and radiation transfer. It can act as condensation nuclei for fog formation that may last for several days or months (Robock, 1991; Nichol, 1997; Legg and Laumonier, 1999; Ward, 1999; Reinhardt et al., 2001). $PM_{2.5}$ is preferentially transported over long distances because these particles are both too small to settle by gravity and too large to coagulate. Furthermore, particles in the

fine fraction are capable of penetrating deeper into the lungs and have been associated with increased mortality and morbidity (Wilson and Spengler, 1996; Pope III et al., 2003; Morris, 2001; Metzger et al., 2004). Despite the importance of $PM_{2.5}$, the $PM_{2.5}$ data is less commonly available than PM_{10} (Walsh and Sherwell, 2011; Chu et al., 2014). Knowing this problem, the World Health Organization (WHO, 2010) proposed a method to obtain annual levels of $PM_{2.5}$ by country, using PM_{10} and $PM_{2.5}/PM_{10}$ ratio.

A better knowledge of the spatial distribution of particulate matter on wildfire events is crucial to understanding the resulting environmental and socio-economic impacts (Martínez et al., 2009; Nunes et al., 2016). In this sense, numerous studies have modeled levels of $PM_{2.5}$ during wildfire events. Among the most important studies are those models that seek to estimate the emissions of $PM_{2.5}$ using different information sources, such as land use, vegetation inventories, types of forest, chemistry analyses, and other information (Wiedinmyer et al., 2006; Hodzic et al. 2007; Martins et al. 2012, Koplitz et al., 2018). The emission estimates of $PM_{2.5}$ in wildfires use a set of fixed source profiles over multiple locations in a period of time. This can result in error even if representative source profiles are used (Wang et al., 2012; Watson et al., 2015; Ying et al., 2018). These limitations can contradict the empirical evidence of ground level monitoring (Lee et al., 2008; Richardson et al., 2018; Majdi et al. 2019).

Alternatively, emissions can be modeled by applying statistical models to particulate matter levels observed at monitoring stations. For instance, Dynamic Linear Models (DLM) are commonly used in air quality modelling and have been widely reviewed (Shaddick and Wakefield, 2002; Cocchi et al., 2007; Cameletti et al., 2011; Fassò and Finazzi, 2011; Sahu, 2012). DLM can be extend over a territory including sites where there are no monitoring stations using the Gaussian Field (GF) principles (Blangiardo et al., 2013). This statistical approach allows one to calibrate and validate the model with empirical evidence of ground level monitoring. However, it is usually used with a large number of monitoring stations to calibrate and then validate the model. For example, Cameletti et al. (2013) presented a daily spatio-temporal model of PM_{10} using 24 stations to calibrate and 10 stations to validate the model. Sahu (2012) presented a dayli maximum 8-hour average ozone levels modelling with 117 monitorins stations to calibrate and 12 stations to validate the proposed model.

Considering that DLM have not been applied and evaluated in wildfires events, this article aims to modelling hourly spatio-temporal evolution of $PM_{2.5}$ concentrations on wildfire event, using DLM with Stochastic Partial Differential Equations (SPDE) as application of GF principles. The proposal is tested with an application to the common situation of a reduced number of monitoring stations available for calibrating and validating the application of the model in a certain region and temporal scale, but with additional stations with PM_{10} observations available. We propose the use of $PM_{2.5}$ observations for model calibration, in a standard way, assuming that the number of stations does not allow for splitting, and the use of additional PM_{10} data for model validation. The approach presented requires the presence of monitoring stations with both $PM_{2.5}$ and PM_{10} data, which connects $PM_{2.5}$ modeling with trends given by data from PM_{10} monitoring stations using the ratio $PM_{2.5}/PM_{10}$. Temporal resolution of both datasets can differ but time spanning should be the same. The case study presented in this work involves one-month with hourly data of 5 monitoring stations for $PM_{2.5}$ and daily data every six days of 6 stations for PM10 with, three stations shared by both data sets. The proposal improves in spatial and temporal scale the method proposed by WHO to obtain $PM_{2.5}$ (WHO, 2010).

The remainder of this article is presented as follows. Section 2 provides the site and wildfire descriptions, datasets used, and a brief background to spatio-temporal model using both DLM and SPDE approaches with their application. Section 3 provides the results. Section 4 provides a discussion, while Section 6 provides the principals conclusions.

2. Data and Methodology

2.1. Site description

Quito is situated in a narrow valley in the Andean mountains at 2,800 m.a.s.l. It has an area of 4,230.6 km^2 and 2,240,000 inhabitants (EMASEO, 2011). The temperature inversions are common events in Quito due to the complex topography and high solar intensity (Jurado and Southgate, 1999). The particulate matter monitoring network in Quito and adjacent areas includes eight stations (Table 1). Five of these eight monitoring stations collected hourly (h) observations of $PM_{2.5}$. Also, six of these eight monitoring stations collected daily observations of PM_{10} every six days (6-d). Location and quality control processes of monitoring stations were stablished by the Environmental Agency of Quito following the criteria for air quality monitoring set by the Environmental Protection Agency of the United States (USEPA) (Secretaria de Ambiente del DMQ, 2017).

Table 1. Main parameters of stations used in the calibration and validation model

Station Name	Location	Elevation (m.a.l.s.)	Pollutants		Station code
For calibration					
Carapungo	78°26'50" W, 0°5'54" S	2851	$PM_{2.5}$ (h)	PM_{10} (6-d)	ST_1
Belisario	78°29'24" W, 0°10'48" S	2835	$PM_{2.5}$ (h)	PM_{10} (6-d)	ST_ 2
Cotocollao	78°29'59,2" W, 0°06'38,8" S	2739	$PM_{2.5}$ (h)	-	ST_3
Centro	78°30'50.4" W, 0°13'17.6" S	2820	$PM_{2.5}$ (h)	-	ST_4
Los Chillos	78°27'18,8" W, 0°17'49,5" S	2453	$PM_{2.5}$ (h)	PM_{10} (6-d)	ST_5
For validation					
Tumbaco	78°24'00" W, 0°12'36" S	2331	-	PM_{10} (6-d)	ST_1V
Tababela	78°20'33" W, 0°11'23" S	2506	-	PM_{10} (6-d)	ST_2V
Jipijapa	78°28'48" W, 0°09'36" S	2781	-	PM_{10} (6-d)	ST_3V

2.2. Wildfire event description

September 2015 was a month when wildfires in Quito were frequent and wide, with 14 September the most outstanding day. In the previous 15 years, no other pollution event had been more remarkable than this one (Espinosa, 2018). Figure 1 shows the complete wildfire event in red colour that occurred on September 2015, for this purpose we used the data product MCD14A1 (Thermal anomalies/Active Fire) from MODIS- Terra/Aqua sensor platform. Additionally, it shows the administrative boundary of Quito (yellow polygon) with the five monitoring stations to calibrate the model (green triangles), and three stations to validate the model (yellow dots).

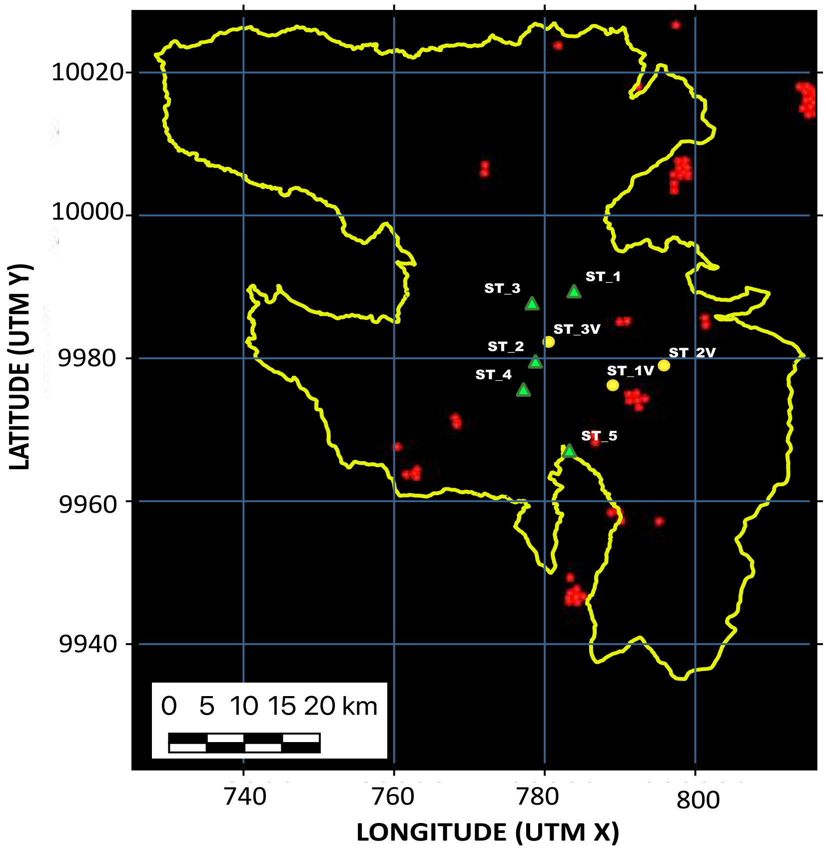

Figure 1. Wildfire event (in red color) on September 2015 (MCD14A1 from MODIS-Terra/Aqua sensor platform) in Quito (yellow polygon), with the monitoring stations to calibrate (green triangles) and validate (yellow dots) the model. The stations labels in the map refer to the “Station code” column in Table 1.

2.3. Data

2.3.1. $PM_{2.5}$ and PM_{10} data

Monitoring hourly values of $PM_{2.5}$ and PM_{10} were compiled from Air Quality Network of Quito for each monitoring site showed in the Table 1. However, the PM_{10} levels were recorded as daily value from 24-h mean every six days. For $PM_{2.5}$ and PM_{10} level data, Thermo Fisher Scientific EPA standard method was used (Zalakeviciute at al., 2019).

2.3.2. Meteorological data

The significant meteorological covariates used in this paper were air temperature (*K*), pressure (mb), radiation ($W{\cdot}m^{-2}$), and surface temperature (*K*). The meteorological data was hourly compiled from the meteorological assimilation system based on satellite data. The Modern-Era Retrospective analysis for Research and Applications version 2 (MERRA-2). MERRA-2 published many analysis products used in atmospheric and air quality modelling (Kuo, 2017; Qin et al., 2018). The results presented in this article are derived from three data products: (1) air temperature (M2I1NXLFO.5.12.4), (2) radiation (M2T1NXRAD.5.12.4), and (3) pressure (M2T1NXSLV.5.12.4). These data products had a spatial resolution of 0.5°×0.625° lat-lon, and temporal resolution of 1 hour. Soil surface temperature variable was used as an indicator of fire events (Bailey and Murray, 1980; Jolly et al., 2015; Liu et al., 2019). This variable (MAT1NXSLV) was hourly collected from MERRA Data Assimilation System 2-Dimensional, using the Goddard Earth Observing System Data Assimilation System Version 5 (GEOS-5 DAS). The soil surface temperature data had a spatial resolution of 0.5°×0.667° lat-lon, and temporal resolution of 1 hour.

2.4. Statistical model: DLM and SPDE approaches.

The dynamic linear modelling approach is described below. Let y_{st} denote the observed generic pollutant concentration at spatial location s ($s = 1, \dots, S$) on hour t ($t = 1, \dots, T$).

If y_{st} denote particulate matter, Blangiardo et al. (2013) suggest applying the natural logarithmic transformation in order to stabilize the variances, and to make the distribution of PM data approximately normal. The observation equation is assumed as

$$y_{st} = X_{st} \cdot \beta + \theta_{st} + v_{st}. \quad (1)$$

In this model, v_{st} represents the measurement error which is assumed to be independent and distributed $N(0, \sigma_v^2)$. The measurement error variance, σ_v^2, also is called the nugget effect (Cressie 1993). The vector β is a vector of regression coefficients and X_{st} represents a vector of regressors that change temporally (large-scale component including meteorological and geographical covariates). For covariates selection in DLM approach, two suggested criteria were used: The Deviance Information Criterion (DIC) defined by Spiegelhalter et al. (2002), and the Watanabe-Akaike Information Criterion (WAIC) introduced by Watanabe (2013), who calls it the widely-applicable information criterion. Gelman et al. (2014) presents a good theoretical explanation of these criteria as well as a historical and analytic comparison between them.

The term θ_{st} is the realization of the latent spatio-temporal process (true unobserved levels of generic pollutant on hour t at site s), and it is a dynamic autoregressive first-order model with coefficient a, given by

$$\theta_{st} = a \cdot \theta_{s,t-1} + w_{st}. \quad (2)$$

The last equation is termed the system equation, and the criteria described by Cameletti et al. (2013) are assumed, with $t = 2, \dots, T$ and $|a| < 1$ and $\theta_{s,1}$ derived from the stationary distribution $N(0, \sigma_w^2/(1-a^2))$. Therefore w_{st} has a normal distribution with zero mean and variance–correlation matrix Σ, $N(0, \Sigma{=}\sigma_w^2\widetilde{\Sigma})$. The dense $S{\times}S$ correlation matrix ($\widetilde{\Sigma}$) uses elements given by the Matérn function, which depends on the Euclidean spatial distance and is parameterized by ρ (for more details, see Cressie 1993, Lindgren et al. 2015, and Cameletti et al. 2013).

For the purpose of spatial prediction of a generic pollutant for sites without monitoring stations, we used the SPDE approach. This uses a finite element representation to define the Mátern field (i.e. a GF with Mátern covariance function, $\theta(s)$) as a linear combination of basis functions defined on a triangulation of the domain *D*. This approach consists of dividing the domain into a set of triangles that do not intersect but are joined only through a vertex. First, the triangulation is generated between the location of the monitoring stations, and then vertices are added to obtain a triangulation that allows spatial predictions (Cameletti et al., 2013). The basis function representation of the Matérn field $\theta(s)$ is given by

$$\theta(s) = \sum_{l=1}^{n} \psi_l(s)\omega_l \qquad (3)$$

where *n* is the vertices number, $\psi_l(s)$ are the basis functions that are chosen to be piecewise linear on each triangle (is 1 at vertex *l* and 0 at all other vertices), and ω_l are Gaussian distributed weights (The height of each triangle, i.e., the value of the spatial field at each triangle vertex). The values in the interior of the triangle are determined by linear interpolation. This representation establishes the link between the Gaussian field $T(s)$ and the Gaussian Markov Random Field (GMRF) defined by the Gaussian weights to which a Markovian structure can be given (for more details, see Lindgren et al., 2015, Cameletti et al., 2013).

2.5. Methodology

The available monitoring stations of $PM_{2.5}$ are used to calibrate the model. The model calibration considers an hourly temporal scale. The model parameters from model calibration are: the vector of regression coefficients (β), the true unobserved logarithmic levels of generic pollutant on day t at station s denoted by θ_{st}, the measurements error variance (σ_v^2), spatial variance (σ_w^2), and the coefficients a and ρ.

As all $PM_{2.5}$ monitoring stations were used in the model calibration, we developed a method for estimating $PM_{2.5}$ concentration at additional validation stations (Walsh and Sherwell, 2011; Chu et al., 2014). A similar approach was proposed by World Health Organization, 2010. Our approach considered the equal or similar behavior of particulate matter between nearby points in local and regional studies (Munir, 2017; Xu et al., 2017; Zhao et al., 2019).

The proposed method had two elements. The first element was the $PM_{2.5}/PM_{10}$ ratio based on the daily mean value of $PM_{2.5}$ calculated for the same days when the daily PM_{10} values were collected (Marcazzan et al., 2011; Chu et al., 2015; Li et al., 2017). The $PM_{2.5}/PM_{10}$ ratio was calculated from monitoring stations that had both $PM_{2.5}$ and PM_{10} observation (termed support stations). This assumption was made considering the equivalent methodology used in the PM monitors. With particulate matter, to accurately compare the data it will need to be from monitors where the agreement is strong enough to be used interchangeably in the model (Mehadi et al., 2019).

The second element was a distance matrix between validation and support stations. The closest support station in the distance matrix was used for each validation station. This analysis allowed us to associate each validation station with a support station. After this analysis, the PM_{10} behavior was evaluated in the associated stations through a correlation analysis (Ito et al., 2001). The correlation analysis allowed us to assign the $PM_{2.5}/PM_{10}$ ratio of a support station to its respective validation station.

Then to estimate the daily $PM_{2.5}$ concentration every six days ($PM^*_{2.5}$) based on the PM_{10} concentration collected every six days ($PM_{10\,(obs)}$) and the $PM_{2.5}/PM_{10}$ ratio assigned to each validation station, we used the Equation 4

$$PM^*_{2.5} = PM_{10\,(obs)}\, x\, \frac{PM_{2.5}}{PM_{10}}. \qquad (4)$$

The model evaluation had two stages: the first stage of evaluating the model calibration, and the second one of evaluating the model validation; for these purposes, the Nash-Sutcliffe Efficiency Index (NSE), root-mean-square error (RMSE), and Pearson correlation coefficient were used. NSE (Eq. 5) is a widely used and potentially reliable statistic for assessing the goodness of fit of models. The NSE scale is from 0 to 1, whereby *NSE = 1* means the model is perfect. *NSE = 0* means that the model is equal to the average of the observed data, and negative values mean that the average is a better predictor (McCuen et al., 2006)

$$NSE = 1 - \frac{\sum(Yobs_i - Ysim_i)^2}{\sum(Yobs_i - \overline{Yobs})^2}. \qquad (5)$$

Unlike RMSE, the NSE and Pearson correlation are independent of the scale of measurement of the variables. $Yobs_i$ denotes the observed hourly $PM_{2.5}$ concentration in the calibration processes, and the daily $PM_{2.5}^{*}$ values in the validation processes. $Ysim_i$ denotes simulated hourly $PM_{2.5}$ concentrations in the calibration processes, and the simulated values of the daily mean $PM_{2.5}$ concentration in the validation processes. The quality metrics for the general model and for each monitoring station were obtained.

3. Results

Our spatio-temporal model was applied to the five monitoring stations (*S=5*) having $PM_{2.5}$ data on hour t (*T=720*). As the SPDE approach is applied on a mesh, the triangulation proposed in this paper has 41 vertices, with each monitoring and validation stations given a vertex. Per Lindgren and Rue (2015), we used a comparative analysis between the results obtained from two meshes: the first one with 41 vertices, and the second one with 219 vertices. In the model calibration, the quality metrics (RMSE, NSE, and Pearson correlation coefficient) were equal for both meshes. The quality metrics were similar for both meshes in the model validation. Thus, the results were not influenced significantly by the mesh selection, and so we can be used the mesh with less number of vertices. We used the mesh with less number of vertices because the computational time required to fit the models are related to mesh size and model complexity at each vertex (Krainski et al., 2018).

Figure 2(a) shows the five monitoring stations and three validation stations (points and triangles, respectively). This process also considered a 26 × 26 grid, with distance between each intersection of 4 *km*; in total, 676 intersections were used. Each intersection point contains 720 recorded data (hourly data during September) for each covariate defined in the model (see Figure 2(b)).

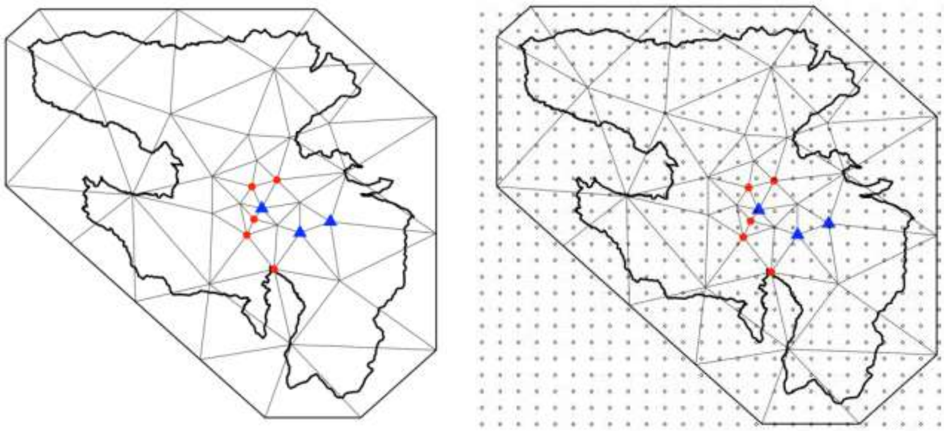

(a) (b)

Figure 2. (a) Triangulation of DMQ region using 41 vertices; (b) 26 × 26 grid with satellite data.

The posterior estimates (mean, quantiles, and standard deviation) for hyperparameters σ_v^2, σ_w^2, ρ and a are shown in Table 2. The spatial variance has the most significant mean value in the proposed model. A similar result was obtained by Cameletti et al. (2013). We obtained a value of 27.190 *km* for the empirically-derived correlation range, which is the distance at which the correlation is close to 0.1. Considering the area of study, it is enough to cover a local territory in which there are limited monitoring stations. The empirically-derived correlation range allows to check if the proposed method for the model validation between two nearby stations can be used.

Table 2. Posterior estimates (mean, standard deviation, and quantiles).

Parameter	Mean	SD	25%	50%	97.5%
σ_v^2	0.1650	0.00748	0.1509	0.1648	0.1803
σ_w^2	0.2645	0.01662	0.2334	0.2639	0.2986
ρ	27.190	1.9358	23.601	27.111	31.198
a	0.7565	0.01851	0.7188	0.7570	0.7914

Table 3 shows the regression coefficients from the spatio-temporal model (mean, standard deviation, and quantiles). The posterior mean of the intercept is 2.751 on the logarithmic scale. The mean value of the intercept means an average of $PM_{2.5}$ concentration of about 16 $\mu g{\cdot}m^{-3}$, after adjusting for covariates.

In the proposed model, the altitude coefficient had the most significant posterior mean value (–0.32): altitude had an inverse influence on logarithmic $PM_{2.5}$ concentration, i.e., the concentration of $PM_{2.5}$ decreases with increasing altitude. This behavior has been widely studied (Viana et al., 2005; Ding et al., 2005; Si-Jia et al., 2016). Further, altitude had an inverse relationship with pressure (Chen et al., 2008). However, the mean value of pressure coefficient (0.04) had no important influence on logarithmic $PM_{2.5}$ concentration.

The mean value of the UTMY coordinate coefficient (0.26) had an important direct influence on the logarithmic $PM_{2.5}$ concentration. This behavior could be associated to forest fire location, as in this work, the most affected zones were in the northern strip. The mean value of air temperature coefficient (–0.24) had an important inverse relation with logarithmic $PM_{2.5}$ concentration. Air temperature and radiation are linked to thermal inversion and air density; thus, the concentration of $PM_{2.5}$ decreases with increasing air temperature and radiation (Hasheminassa et al., 2014).

The mean value of surface temperature had less influence on the logarithmic $PM_{2.5}$ concentration. However, the surface temperature had a positive relationship with the concentration of $PM_{2.5}$; in other words, the concentration of $PM_{2.5}$ increases with increasing the surface temperature (Ward and Smith, 2005; Luhar et al., 2008, Gaetani et al., 2012).

Table 3. Regression coefficients (mean, standard deviation, and quantiles)

Covariate	Mean	SD	2.5%	50%	97.5%
Intercept	2.751	0.04	2.67	2.752	2.83
Altitude	-0.3237	0.05	-0.42	-0.32371	-0.223
UTMX	-0.08401	0.04	-0.16	-0.08400	-0.003
UTMY	0.26322	0.03	0.19	0.26321	0.33
Air Temp.	-0.23953	0.04	-0.31	-0.23952	-0.16
Pressure	0.03791	0.01	0.01	0.03792	0.064
Radiation	-0.1118	0.03	-0.17	-0.11179	-0.047
Surface Temp.	0.0444	0.03	-0.01	0.0443	0.107

Overall, the model calibration had an NSE of 0.83, an RMSE of 0.32, and a Pearson correlation coefficient of 0.92. These values show a good quality model and fitted values in the calibration stage (Ritter and Muñoz-Carpena, 2013). The quality model and fitted values for each monitoring stations at the calibration stage presented a similar behavior; the values obtained are showed in Table 4.

Table 4. Quality analysis for each monitoring station

Parameter	EST_1	EST_2	EST__3	EST_4	EST_5
NSE	0.82	0.79	0.80	0.81	0.82
RMSE	0.24	0.32	0.26	0.39	0.37
Pearson Correlation Coeff.	0.92	0.89	0.90	0.91	0.92

The model validation used the $PM_{2.5}/PM_{10}$ calculated at three monitoring stations: ST_1: Carapungo, ST_2: Belisario, and ST_5: Los Chillos. Figure 3 shows the $PM_{2.5}/PM_{10}$ ratio behavior on the time (every six days) at support stations.

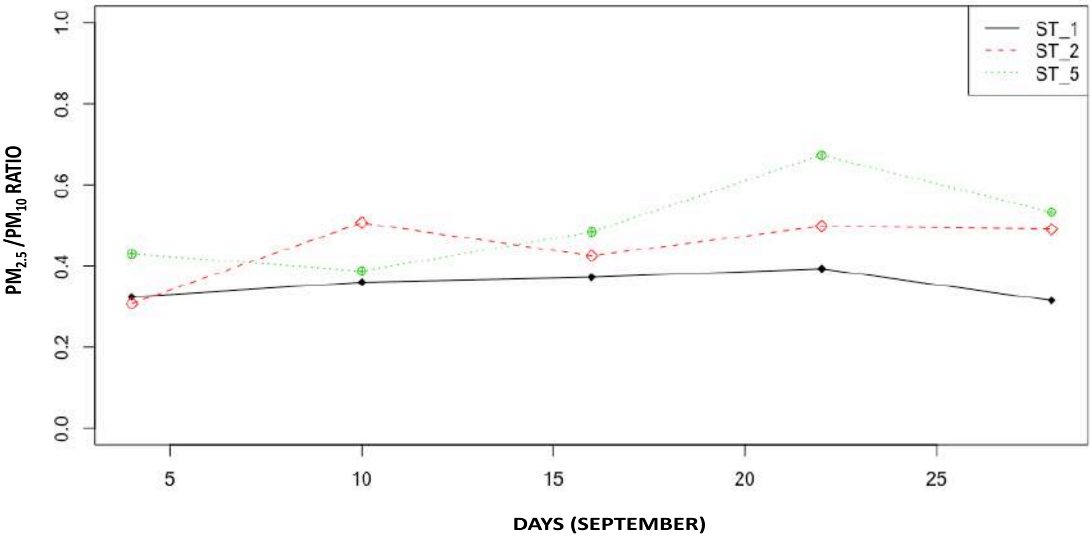

Figure 3. $PM_{2.5}/PM_{10}$ ratio obtained every six days at support stations.

Overall, ST_1 had the lowest $PM_{2.5}/PM_{10}$ ratio and the ST_5 had the highest ratio. The north of DMQ has more influence on PM_{10}, while the south was influenced by $PM_{2.5}$. Díaz and Pérez (2006) have explained that this behavior is due to the wind direction, as the wind crosses the territory from north to south.

The second element for the validation model in our case study was the distance matrix between validation and support stations. It is showed in the Table 5.

Table 5. Distance matrix between validation and support stations in *km*

	ST_1V	ST_2V	ST_3V
ST_1	14.161	15.851	7.882
ST_2	10.806	17.069	3.217
ST_3	15.728	19.572	5.871
ST_4	11.872	18.944	7.427
ST_5	10.763	17.265	15.406

The associated stations were: ST_1V with ST_5, ST_2V with ST_1, and ST_3V with ST_2. As shown in Table 6, the PM_{10} correlation analysis of the associated stations gave adequate correlation coefficients (R^2). These adequate correlations allowed us to assign the $PM_{2.5}/PM_{10}$ ratio from support stations to validation stations.

Table 6. Associated stations and their correlation coefficients

Validation station	Support station	Correlation Coefficient (R2)	Linear equation
ST_1V	ST_5	0.697	$PM_{10:\,ST\_1V} = 0.8432 \cdot PM_{10:\,ST5} + 10.288$

ST_2V	ST_1	0.999	$PM_{10:ST\_2V} = 1.5586 \cdot PM_{10:ST1} - 75.715$
ST_3V	ST_2	0.966	$\mathrm{PM}_{10:\mathrm{ST\_3V}} = 0.75 \cdot \mathrm{PM}_{10:\mathrm{ST2}} + 11.45$

The model validation in general had a Nash-Sutcliffe efficiency index of 0.50, an RMSE of 0.16, and a Pearson correlation coefficient of 0.78. The model proposed by Cameletti et al. (2013) to predict PM_{10} with a daily scale had the next quality metrics: an RMSE of 0.5328, with a correlation coefficient of 0.7015, using a direct validation method at a large number of monitor stations to calibrate and validate the model.

Table 7 shows the quality indices per each validation site. The validation site ST_2V presented the lowest NSE value (i.e., for this validation site will be better take the mean value to predict).

Table 7. Quality analysis for each validation point

Parameter	ST_1V	ST_2V	ST_3V
NSE	0.28	-2.1	0.94
RMSE	0.17	0.208	0.02
Pearson Correlation Coeff.	0.78	0.79	0.99

In the wildfire described in this work, the affected areas corresponded to the identified areas of recurrence of wildfires by Columba et al. (2016). In this work the most affected area by wildfire were located in the north. Four sites in the territory were randomly selected. Figure 4 shows the hourly behavior of logarithmic $PM_{2.5}$ concentration in September 2015 at randomly selected four sites at which there are no monitoring stations. Figure 4 shows high logarithmic $PM_{2.5}$ concentrations in the central and north zones of DMQ (Site 1, Site 2, and Site 3), and low concentrations in the south of Quito (Site 4). Wildfires during September were continuous at different territorial extensions and intensities. The largest wildfires started on September 6, 14, and 28. The curves shown in the Figure 4 presented slight peaks around the indicated dates. However, the spikes are not noticeable due to the location of monitoring stations near to the paths in the urban area, and they can recorder levels of anthropogenic fine particulate matter, such as emissions from diesel vehicles. The dynamic presented in the Figure 4 is specifically intraday (hourly).

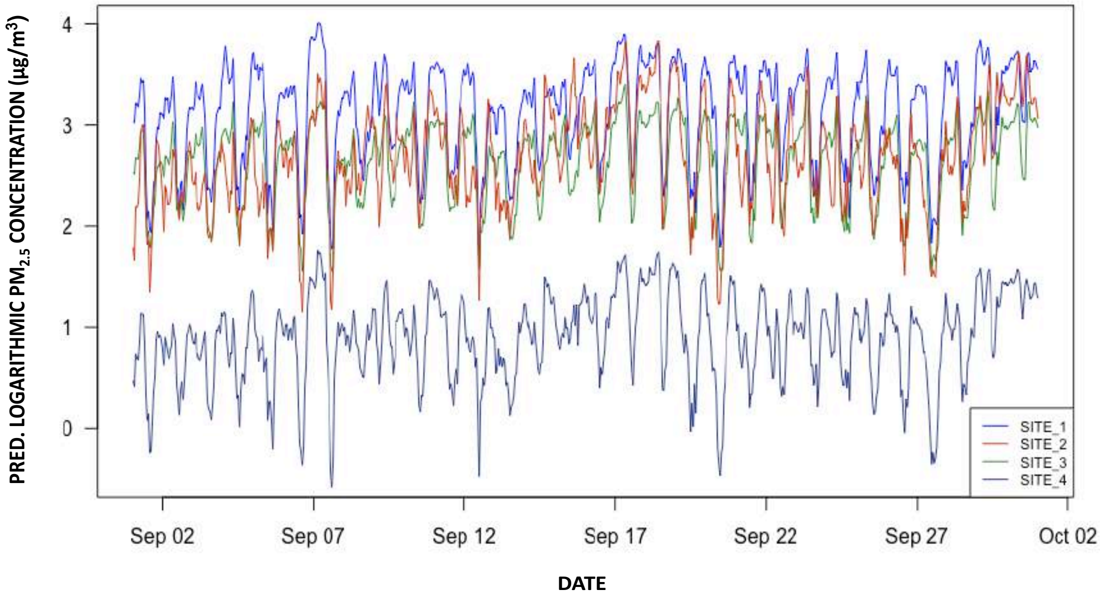

Figure 4. Hourly logarithmic $PM_{2.5}$ concentrations ($\mu g/m^3$) at unknown pollution sites.

Figure 5 shows the spatial logarithmic concentrations for $PM_{2.5}$ at two times on 14 September 2015 (the most outstanding wildfire), for which MODIS information was available directly. We used the data product MOD14A1 (Thermal anomalies/Active Fire) from MODIS-Terra sensor platform in the morning (10h30), and MYD14A1 (Thermal anomalies/Active Fire) from MODIS-Aqua sensor platform in the afternoon (13h30). In two cases, the high levels of $PM_{2.5}$ were located in the northwest of Quito. The main reason for this is that the fire magnitude in the north was larger and more prolonged than in the center and south area at Quito. Figure 6 shows the highest hourly logarithmic concentration of $PM_{2.5}$ at the most outstanding wildfire (14 September 2015, 16:00).

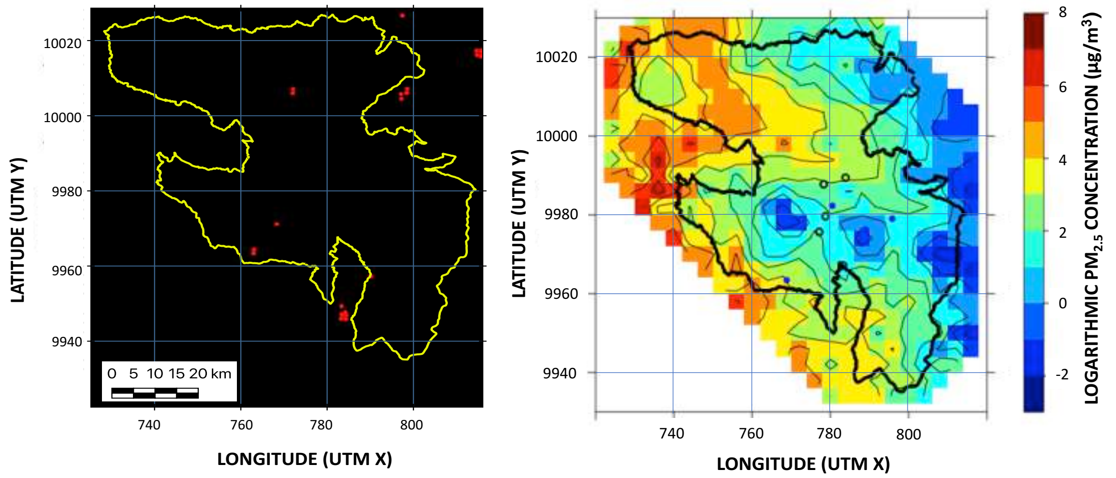

(a)

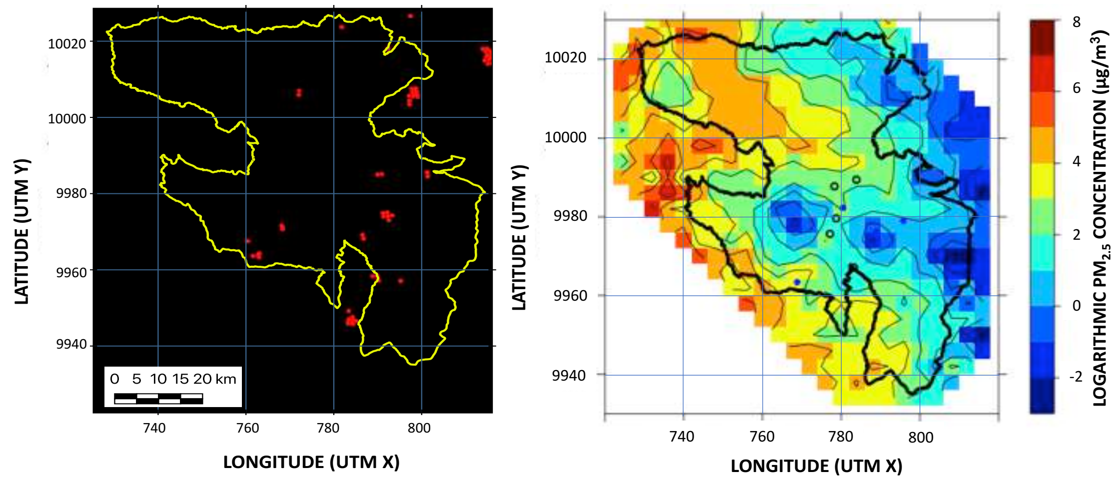

(b)

Figure 5. (a) Thermal anomalies/Active Fire (MOD14A1 from MODIS-Terra) at 10h30 (left), and the predicted logarithmic $PM_{2.5}$ concentration at 11h00 (right) on 14 September; (b) Thermal anomalies/Active Fire (MYD14A1 from MODIS-Aqua) at 13h30 (left), and the predicted logarithmic $PM_{2.5}$ concentration at 14h00 (right) on 14 September.

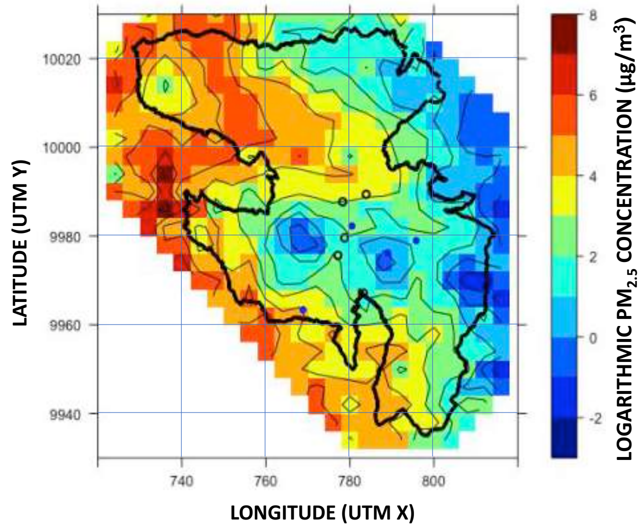

Figure 6. Model results on 14 September at 16:00 (maximum level, global analysis)

4. Discussion

The soil surface temperature variable with hourly temporal resolution (MAT1NXSLV from MERRA Data Assimilation System 2-Dimensional) was used in the proposed model as an indicator of fire events; despite the proper behavior of the model, the main limitation of this variable is that it cannot distinguish between recently extinguished and active wildfires. Thermal Anomalies/Active Fire products from MODIS (Terra: MOD14A1, Aqua: MYD14A1, and Terra-Aqua: MCD14A1) could be used in further studies as indicator of wildfire on the proposed model. However, Thermal Anomalies/Active Fire products have high spatial resolution but low temporal resolution. For this reason, in further studies is necessary use complementary spatio-temporal models of Thermal Anomalies/Active Fire with hourly resolution developed in the last years. The (Veraverbeke et al., 2014; Xie et al., 2018; Yao et al., 2018; Ban et al., 2020).

The spatial resolution of ground-based monitoring records generally is not sufficient for the management of risks associated with wildfires, however we proposed a validation method to estimate daily $PM_{2.5}$ concentration in local territories using available daily data of PM_{10} and $PM_{2.5}$/ PM_{10} ratio from support stations. An hourly resolution data of PM_{10} and $PM_{2.5}$/ PM_{10} ratio could be used in further studies. Alternatively, satellite images of variables related to $PM_{2.5}$, such as Aerosol Optical Depth (AOD), can provide a valuable alternative to the coarse spatial resolution of ground monitoring network measurements (Kumar et al., 2013; Xie et al., 2015, Ma et al., 2016; Geng et al., 2018). Numerous statistical approaches have been used to estimate the relationship between AOD and $PM_{2.5}$ with daily resolution, however, due to hourly-varying meteorological variables, that relationship changes over time and space. Hence, it is required use approaches with high temporal resolutions (Liu et al., 2019; Mirzaei et al., 2020). Thermal Anomalies/Active

Fire and AOD data must have the appropriate temporal (hourly) and spatial resolution (less than 0.25º) to calibrate and validate the proposed model. Additionally, it must to considering the principals temporal and spatial limitations (e.g. cloud obscuration) (Ying et al., 2018; Zhang et al., 2018).

5. Conclusions

An air quality model was developed to obtain the hourly spatio-temporal behavior of $PM_{2.5}$ on a wildfire event using few monitoring stations. An advantage of our model is the low computational cost required, which can be beneficial for a swift response against of the environmental and health risk. To overcome the limitation of few monitoring stations, we have developed a novel method to validate the model. The validation method presented here produced adequate quality metrics that are comparable to the direct methods. The validation model proposed in this article worked well in a local scale on daily temporal scale, where the behavior of particulate matter is similar between two nearby points; and the spatial variation of the meteorological covariates is slight in a small city. The validation method proposed in this work improves the method by the World Health Organization to obtain $PM_{2.5}$ levels in cities and localities in Latin America and the Caribbean. Because they use a regional $PM_{2.5}/PM_{10}$ ratio with annual periodicity

Our model proposed is capable of describing $PM_{2.5}$ pollution levels in places where there are no monitoring stations, under the conditions of a wildfire as determined by satellite information. The proposed model to determine $PM_{2.5}$ levels in wildfire event can be an interesting tool for managing environmental and health risks.

Declaration of competing interest

The authors declare that they have no known competing financial interest or personal relationships that could have appeared to influence the work reported in this paper.

Acknowledgments

We acknowledge and thank authorities of Red Metropolitana de Monitoreo Atmosférico de Quito (REMMAQ) for providing complementary information to this work. Joseph Sánchez Balseca is the recipient of a full scholarship from the Secretaria de Educación Superior, Ciencia, Técnología e Innovación (SENESCYT), Ecuador.

Data Availability

Datasets related to this article can be found at http://190.11.24.212/reportes/ReporteHorariosData.aspx, an open-source online data repository hosted at Secretaria de Ambiente del Distrito Metropolitano de Quito (Secretaria de Ambiente DMQ, 2015).

Bibliography

Akaike, H. (1973). Information theory and an extension of the maximum likelihood principle. *Proceedings of the Second International Symposium on Information Theory* (págs. 267–281). Budapest: B. N. Petrov and F. Csaki.

Amraoui, M., Pereira, M., DaCamara, C., & Calado, T. (2015). Atmospheric conditions associated with extreme fire activity in the Western Mediterranean region. *Science of the Total Environment, 524-525*, 32-39.

Ando, T. (2007). Bayesian predictive information criterion for the evaluation of hierarchical Bayesian and empirical Bayes models. *Biometrika, 94*(2), 443–45.

Bailey, A., & Murray, A. (1980). Fire Temperatures in Grass, shrub and Aspen Forest Communities of Central Alberta. *Journal of range management , 33*(1), 37-40.

Ban, Y., Zhang, P., Nascetti, A., Bevington, A., & Wulder, M. (2020). Near Real-Time Wildfire Progression Monitoring with Sentinel-1 SAR Time Series and Deep Learning. *Scientific Reports*, *10*(1322), 1-15.

Blangiardo, M., Cameletti, M., Baio, G., & Rue, H. (2013). Spatial and spatio-temporal models with R-INLA. *Spatial and Spatio-temporal Epidemiology*, 33–49.

Blangiardo, M., Pirani, M., Kanapka, L., Hansell, A., & Fuller, G. (2018). A hierarchical modelling approach to assess multi pollutant effects in time-series studies. *Cornell University*.

Bravo, A., Sosa, E., Sánchez, A., Jaimes, P., & Saavedra, R. (2002). Impact of wildfires on the air quality of Mexico City, 1992–1999. *Environmental Pollution*, 243-253.

Cameletti, M., Ignaccolo, R., & Bande, S. (2011). Comparing spatio-temporal models for particulate matter in Piemonte. *Environmetrics, 22*(8), 985–996.

Cameletti, M., Lindgren, F., Simpson, D., & Rue, H. (April de 2013). Spatio-temporal modeling of particulate matter concentration through the SPDE approach. *AStA Advances in Statistical Analysis, 97*(2), 109–131.

Cocchi, D., Greco, F., & Trivisano, C. (2007). Hierarchical space-time modelling of PM10 pollution. *Atmospheric Environment*, 532-542 .

Columba, M. J., Quisilema, W., Padilla, O., & Toulkeridis, T. (2016). Identificación las zonas de recurrencia de incendios forestales mediante análisis multitemporal y aplicación de índices espectrales, en el Distrito Metropolitano de Quito. *Revista de Ciencias de Seguridad y Defensa, 1*(3), 7-13.

Cressie, N. (1993). *Statistics for Spatial Data, Revised Edition.* Michigan: John Wiley & Sons.

Chen, Z., Cheng, S., Li, J., Guo, X., Wang, W., & Chen, D. (2008). Relationship between atmospheric pollution processes and synoptic pressure patterns in northern China. *Atmospheric Environment, 42*, 6078– 6087.

Chu, H.-J., Huang, B., & Lin, C.-Y. (2014). Modeling the spatio-temporal heterogeneity in the PM_{10}-$PM_{2.5}$ relationship. *Atmospheric Environment, 102*, 176-182.

Díaz, V., & Páez, C. (2006). Contaminación por material particulado en Quito y caracterización química de las muestras. *Acta Nova, 3*(2), 308-322.

Ding, G., Chan, C., Gao, Z., Yao, W., Li, Y., Cheng, X., Miao, Q. (2005). Vertical structures of PM_{10} and $PM_{2.5}$ and their dynamical character in low atmosphere in Beijing urban areas. *Science in China Series D Earth Sciences*(48), 38-54.

EMASEO. (2011). *Plan de Desarrollo 2012-2022.* Municipio del Distrito Metropolitano de Quito. Quito: Municipio del Distrito Metropolitano de Quito.

Espinosa, K.-G. (2018). *Inventario de emisiones atmosféricas producidas por incendios forestales en el Distrito Metropolitano de Quito. Septiembre de 2015.* Quito: Universidad San Francisco de Quito.

Fann, N., Alman, B., Broome, R., Morgan, G., Johnston, F., Pouliot, G., & Rappold, A. (2018). The health impacts and economic value of wildland fire episodes in the U.S.: 2008–2012. *Science of the Total Environment, 610-611*, 802-809.

Fassò, A., & Finazzi, F. (2011). Maximum likelihood estimation of the dynamic coregionalization model with heterotopic data. *Environmentrics*, 735-748.

Gaetani, M., Pasqui, M., Criscia, A., & Guarnieri, F. (2012). A synoptic characterization of the dust transport and associated thermal anomalies in the Mediterranean basi. *International Journal of Climatology*(7), 2779-2791.

Gelman, A., Hwang, J., & Vehtari, A. (2014). Understanding predictive information criteria for Bayesian models. *Statistics and Computing*, 997–1016.

Geng, G., Murray, N., Tong, D., Fu, J., Hu, X., Lee, P., . . . Liu, Y. (2018). Satellite-based daily PM2.5estimates during fire seasons in Colorado. *Journal of Geophysical Research: atmospheres, 123*(15), 8159-8171.

Haiganoush, P., Schweizer, D., Cisneros, R., Procter, T., Ruminski, M., & Tarnay, L. (2015). A statistical model for determining impact of wildland fires on Particulate Matter (PM2.5) in Central California aided by satellite imagery of smoke. *Environmental Pollution*, 340-349.

Hasheminassa, S., Pakbin, P., Delfino, R. J., Schauer, J. J., & Sioutasa, C. (2014). Diurnal and seasonal trends in the apparent density of ambient fine and coarse particles in Los Angeles. *Environmental Pollution*, 1-9.

Hirschberger, P. (2016). *Forest ablaze: causes and effects of global forest fires.* Berlin, Germany: WWF Deutschland.

Hodzic, A., Madronich, S., Bohn, B., Massie, S., Menut, L., & Wiedinmyer, C. (2007). Wildfire particulate matter in Europe during summer 2003: meso-scale modeling of smoke emissions, transport and radiative effects. *Atmospheric Chemistry and Physics*, 4043–4064.

Ito, K., Thurston, G., Nádas, A., & Lippmann, M. (2001). Monitor-to-monitor temporal correlation of air pollution and weather variables in the North-Central U.S. *Journal of Exposure Analysis and Environmental Epidemiology*(11), 21-32.

Jolly, M., Cochrane, M., Freeborn, P., Holden, Z., Brown, T., Williamson, G., & Bowman, D. (2015). Climate-induced variations in global wildfire danger from 1979 to 2013. *Nature Communications, 6*(7537).

Jurado, J., & Southgate, D. (1999). Dealing with air pollution in Latin America: thecase of Quito, Ecuador. *Environment and Development Economics*, 375–388.

Knorr, W., Lehsten, V., & Arneth, A. (2012). Determinants and predictability of global wildfire emissions. *Atmospheric Chemistry and Physics, 12*(15), 6845-6861.

Koplitz, S., Nolte, C., Pouliot, G., Vukovich, J., & Beidlerc, J. (2018). Influence of uncertainties in burned area estimates on modeled wildland fire $PM_{2.5}$ and ozone pollution in the contiguous U.S. *Atmospheric Environment, 191*, 328-339.

Krainski, E. T., Gómez-Rubio, V., Bakka, H., Lenzy, A., Castro-Camilo, D., Simpson, D., Rue, H. (2018). *Advanced Spatial Modeling with Stochastic Partial Differential Equations Using R and INLA.* Trondheim, Norway: Chapman and Hall/CRC .

Kumar, R., Sivakumar, V., Reddy, R., Gopal, R., & Adesina, J. (2013). Inferring wavelength dependence of AOD and Ångström exponent over a sub-tropical station in South Africa using AERONET data: Influence of meteorology, long-range transport and curvature effect. *Science of The Total Environment*, 397-408.

Kuo, C.-L. (2017). Assessments of Ali, Dome A, and Summit Camp for mm-wave Observations Using MERRA-2 Reanalysis. *The Astrophysical Journal, 848*(1), 1-11.

Lee, S., Kim, H., Yan, B., Cobb, C., Hennigan, C., Nichols, S., Russell, A. (2008). Diagnosis of Aged Prescribed Burning Plumes Impacting an Urban Area. *Environmental Science & Technology, 42*(5), 1438-1444.

Legg, C. A., & Laumonier, Y. (1999). Fires in Indonesia, 1997: A remote sensing perspective. *Ambio, 28*(6), 479-485.

Li, L., Wu, A., Cheng, I., Chen, J.-C., & Wu, J. (2017). Spatiotemporal estimation of historical $PM_{2.5}$ concentrations using PM_{10}, meteorological variables, and spatial effect. *Atmospheric Environment, 166*, 182-191.

Lindgren, F., & Rue, H.˚. (2015). Bayesian Spatial Modelling with R-INLA. *Journal of Statistical Software*, 1-25.

Liu, Z., Ballantyne, A., & Cooper, A. (2019). Biophysical feedback of global forest fires on surface temperature. *Nature communications, 10*(214).

Liu, J., Weng, F., Li, Z., & Cribb, M. (2019). Hourly PM2.5 Estimates from a Geostationary Satellite Based on an Ensemble Learning Algorithm and Their Spatiotemporal Patterns over Central East China . Remote sensing, 11(18), 2120.

Luhara, A. K., Mitchell, R. M., Meyera, C. (., Qin, Y., Campbell, S., Grasa, J. L., & Parry, D. (2008). Biomass burning emissions over northern Australia constrained by aerosol measurements: II—Model validation, and impacts on air quality and radiative forcing. *Atmospheric Environment* (42), 1647–1664.

Ma, X., Wang, J., Yu, F., Jia, H., & Hu, Y. (2016). Can MODIS AOD be employed to derive $PM_{2.5}$ in Beijing-Tianjin-Hebei over China? *Atmospheric Research*, 250-256.

Majdi, M., Turquety, S., Sartelet, K., Legorgeu, C., Menut, L., & Kim, Y. (2019). Impact of wildfires on particulate matter in the Euro-Mediterranean in 2007: sensitivity to some parameterizations of emissions in air quality models. *Atmospheric Chemistry and Physics.*, 785–812.

Manta, M., & Sanhueza, P. (2015). Wildfires in South America. *Crisis Response*, 56-57.

Marcazzan, G., Vaccaro, S., Valli, G., & Vecchi, R. (2001). Characterisation of PM_{10} and $PM_{2.5}$ particulate matter in theambient air of Milan (Italy). *Atmospheric Environment, 35*, 4639–4650.

Martínez, J., Vega-Garcia, C., & Chuvieco, E. (2009). Human-caused wildfire risk rating for prevention planning in Spain. *Journal of Environmental Management, 90*(2), 1241-1252.

Martins, V., Miranda, A., Carvalho, A., Schaap, M., Borrego, C., & Sá, E. (2012). Impact of forest fires on particulate matter and ozone levels during the 2003, 2004 and 2005 fire seasons in Portugal. *Science of the Total Environment*, 53–62.

Mathur, R. (2008). Estimating the impact of the 2004 Alaskan forest fires on episodic particulate matter pollution over the eastern United States through assimilation of satellite-derived aerosol optical depths in a regional air quality model. *Journal of Geophysical Research*, 1-14.

McCuen, R. H., Knight, Z., & Cutter, A. G. (2006). Evaluation of the Nash–Sutcliffe Efficiency Index. *Journal of Hydrologic Engineering*, *11*(6), 597-602.

Mehadi, A., Moosmüller, H., Campbell, D., Ham, W., Schweizer, D., Tarnay, L., & Hunter, J. (2019). Laboratory and Field Evaluation of Real-time and Near Real-time PM2.5 Smoke Monitors. *Journal of the Air & Waste Management Association*.

Metzger, K. B., Tolbert, P. E., Klein, M., Peel, J. L., Flanders, W. D., Todd, K., Frumkin, H. (2004). Ambient air pollution and cardiovascular emergency departament visits. *Epidemiology, 15*(1), 46-56.

Mirzaei, M., Bertazzon, S., Couloigner, I., Farjad, B., & Ngom, R. (2020). Estimation of local daily PM2.5 concentration during wildfire episodes: integrating MODIS AOD with multivariate linear mixed effect (LME) models. *Air Quality, Athmosphere & Health, 13*, 173-185.

Morris, R. D. (2001). borne particulates and hospital admissions for cardiovascular disease: a quantitative review of the evidence. *Enviroment Health Perspective, 109*(4), 495-500.

Munir, S. (2017). Analysing Temporal Trends in the Ratios of $PM_{2.5}/PM_{10}$ in the UK. *Aerosol and Air Quality Research*(17), 34-48.

Nichol, J. (1997). Bioclimatic impacts of the 1994 smoke haze event in Southeast Asia. *Atmospheric Environment, 31*(8), 1209-1219.

Nunes, A., Lourenço, L., & Castro-Meira, A. (2016). Exploring spatial patterns and drivers of forest fires in Portugal (1980–2014). *Science of the Total Environment, 573*, 1190-1202.

Pope III, C., Burnett, R., & Thun, M. (2003). Cardiopulmonary Mortality, and Long-term Exposure to Fine Particulate Air Pollution. *JAMA*, 1132–1141.

Qin, W., Zhang, Y., Chen, J., Yu, Q., Cheng, S., Li, W., Tian, H. (2018). Variation, sources and historical trend of black carbon in Beijing, China based on ground observation and MERRA-2 reanalysis data. *Environmental Pollution, 245*, 853-863.

Reinhardt, E., Ottmar, R., & Castilla, C. (2001). Smoke impacts from agricultural burning in a rural Brazilian town. *Air Waste Manage, 51*(4), 43-50.

Richardson, C., Rutherford, S., & Agranovski, I. (2018). Characterization of particulate emissions from Australian open-cut coal mines: Toward improved emission estimates. *Journal of the Air & Waste Management Association , 68*(6), 598-607.

Ritter, A., & Muñoz-Carpena, R. (2013). Performance evaluation of hydrological models: Statistical significance for reducing subjectivity in goodness-of-fit assessments. *Journal of Hydrology*, 33-45.

Robock, A. (1991). Surface cooling due to forest fire smoke. *Journal of Geophysical Research Atmospheres, 96*, 20869-20878.

Sahu, S. (2012). *Handbook of Statistics - Hierarchical Bayesian Models for Space–Time Air Pollution Data.* Southampton: Elsevier.

Sapkota, A., Symons, M., Kleissl, J., Wang, L., Parlange, M., Ondov, J., Buckley, T. (2005). Impact of the 2002 Canadian forest fires on particulate matter air quality in Baltimore city. *Environmental Science & Technology*(39), 24-32.

Secretatia de Ambiente del DMQ*, Reporte de calidad del aire, especies medidas, 2015.* http://190.11.24.212/reportes/ReporteHorariosData.aspx.

Secretaria de Ambiente del DMQ. (2017). *Informe de la calidad de aire - 2016.* Quito, Pichincha, Ecuador: Distrito Metropolitano de Quito.

Shaddick, G., & Wakefield, J. (2002). Modelling Daily Multivariate Pollutant Data at Multiple Sites. *Journal of the Royal Statistical Society*, 351-372.

Si-Jia, L., Dongsheng, W., Xiao-Bing, L., Zhanyong, W., Ya, G., & Zhong-Ren, P. (2016). Three-dimensional distribution of fine particulate matter concentrations and synchronous meteorological data measured by an unmanned aerial vehicle (UAV) in Yangtze River Delta, China. *Athmospheric Measurement Techniques*.

Smith, W. (1990). *Air Pollution and Forest.* New Haven: Springer.

Spiegelhalter, D., Best, N., Carlin, B., & van der Linde, A. (2002). Bayesian measures of model complexity and fit. *Journal Royal Statistical Society, 64*(4), 583-639.

Veraverbeke, S., Sedano, F., Hook, S., Randerson, J., Jin, Y., & Rogers, B. (2014). Mapping the daily progression of large wildlandfires using MODIS active fire data. *International Journal of Wildland Fire*, *23*, 655-667.

Viana, M., Pérez, C., Querola, X., Alastueya, A., Nickovicc, S., & Baldasano, J. (2005). SpatialandtemporalvariabilityofPMlevelsand composition in a complex summer atmospheric scenario in Barcelona (NE Spain). *Atmospheric Environment* (39), 5343-5361.

Walsh, K., & Sherwell, J. (2011). Estimation of Ambient $PM_{2.5}$ Concentrations in Maryland and Verification by Measured Values. *Journal of the Air & Waste Managment Association, 52*(10), 1161-1175 .

Wang, X., Watson, J., Chow, J., Gronstal, S., & Kohl, S. (2012). An Efficient Multipollutant System for Measuring Real-World Emissions from Stationary and Mobile Sources. *Aerosol and Air Quality Research*, 145-160.

Ward, D. (1999). Smoke From Wildland Fires. *Health Guidelines for Vegetation Fire Events* (págs. 70-85). Lima: WHO.

Ward, T. J., & Smith, G. C. (2005). The 2000/2001 Missoula Valley $PM_{2.5}$ chemical mass balance study, including the 2000 wildfire season—seasonal source apportionment. *Atmospheric Environment* (39), 709–717.

Watanabe, S. (2013). A Widely Applicable Bayesian Information Criterion. *Journal of Machine Learning Research*, 867-897.

Watson, J., Chow, J., Lowenthal, D., Chen, A., Shaw, S., Edgerton, E., & Blanchard, C. (2015). $PM_{2.5}$ source apportionment with organic markers in the Southeastern Aerosol Research and Characterization (SEARCH) study. *Journal of the Air & Waste Management Association, 65*(9), 1104-1118.

Wiedinmyera, C., Quayleb, B., Geronc, C., Belotea, A., McKenzied, D., Zhange, X., Klos, K. (2006). Estimating emissions from fires in North America for air quality modeling. *Atmospheric Environment*, 3419–3432.

Wilson, R., & Spengler, J. (1996). *Particles in Our Air.* Massachusetts: Harvard University Physics Department.

World Health Organization. (2010). *World Health Organization.* Recuperado el 24 de December de 2019, de Environmental Statistics and Indicators: Level of concentration of fine particulate matter ($PM_{2.5}$):

http://interwp.cepal.org/sisgen/Sisgen_MuestraFicha_puntual.asp?indicador=3364&id_estudio=952&id_aplicacion=22&idioma=i

Xie, Z., Song, W., Ba, R., Li, X., & Xia, L. (2018). A Spatiotemporal Contextual Model for Forest FireDetection Using Himawari-8 Satellite Data. *Remote Sensing*, 10, 1-24.

Xie, Y., Wang, Y., Zhang, K., Dong, W., Lv, B., & Bai, Y. (2015). Daily Estimation of Ground-Level PM2.5 Concentrations over Beijing Using 3 km Resolution MODIS AOD. *Environmental Science & Technology, 49*(20), 12280-12288.

Xu, G., Jiao, L., Zhang, B., Zhao, S., Yuan, M., Gu, Y., Xin, T. (2017). Spatial and Temporal Variability of the $PM_{2.5}$/PM_{10} Ratio in Wuhan, Central China. *Aerosol and Air Quality Research*(17), 741-751.

Yao, J., Brauer, M., Raffuse, S., & Henderson, S. (2018). A machine learning approach to estimate hourly exposure to fine particulate matter for urban, rural, and remote populations during wildfire seasons. *Environmental Science & Technology*, *52*(22), 13239-13249.

Ying, Q., Feng, M., Song, D., Wu, L., Hu, J., Zhang, H., Li, X. (2018). Improve regional distribution and source apportionment of $PM_{2.5}$ trace elements in China using inventory-observation constrained emission factors. *Science of The Total Environment, 624*, 355-365.

Zalakeviciute, R., Rybarczyk, Y., Granda-Albuja, M. G., Diaz, M. V., & Alexandrino, K. (2019). Chemical characterization of urban PM_{10} in the Tropical Andes. *Atmospheric Pollution Research*.

Zhang, T., Zhu, Z., Gong, W., Zhu, Z., Sun, K., Wang, L., Xu, K. (2018). Estimation of ultrahigh resolution PM2.5 concentrations in urban areas using 160 m Gaofen-1 AOD retrievals. Remote Sensing of Environment, 216, 91-104.